APPLIED SCIENCES AND ENGINEERING

How to run 50% faster without external energy

Amanda Sutrisno and David J. Braun*

Technological innovations may enable next-generation running shoes to provide unprecedented mobility. But how could a running shoe increase the speed of motion without providing external energy? We found that the top speed of running may be increased more than 50% using a catapult-like exoskeleton device, which does not provide external energy. Our finding uncovers the hidden potential of human performance augmentation via unpowered robotic exoskeletons. Our result may lead to a new-generation of augmentation devices developed for sports, rescue operations, and law enforcement, where humans could benefit from increased speed of motion.

INTRODUCTION

The top speed of human running, 12.3 m/s (*1*), is near half the top speed of cycling, 21.4 m/s (*2*), despite both motions being human powered. The lower speed of running suggests that humans have untapped energy-supplying capability, which can be used in cycling but cannot be used for faster running. Cycling is faster than running partly because (i) the rolling motion of the wheels prevents collisional energy losses from stepping (*3*) but also because (ii) wheels can support the weight of the body in place of the legs (*4*, *5*), while (iii) pedals enable the human to supply energy continuously in the air (*5*) instead of intermittently when the leg is on the ground (*6*). These three features enable the bicycle to double the top speed of running, despite supplying no external energy and adding weight to the human. The same features may lead to novel augmentation devices that could increase the running speed using untapped human power, without wheels or external energy.

Humans have attempted to surpass their natural running capability using springs for at least a century (*7*, *8*). Springs cannot provide external energy but have been shown to reduce the energy cost of walking by 7.2 ± 2.6% (*9*), running by 4% (*10*) to 8 ± 1.5% (*11*), and jumping by 24% (*12*). However, the current top speed of augmented running, 11 m/s, achieved using a spring prosthesis in series with the legs (*13*), is 10% below the top speed of natural running. A spring in series with the legs can mitigate collisional energy losses but requires the legs to provide a large force to support the body, unlike the wheel of a bicycle (*10*, *13*, *14*). A spring in parallel with the legs can support the body and therefore enable the human to use all the leg force to push against the ground and accelerate (*15*, *16*). However, regardless of whether a spring is used in series or in parallel with the legs, the ground contact time is reduced to 0.1 s at the top speed of natural running (*1*), which severely limits the amount of energy the legs can supply in high-speed running (*6*, *17*–*20*). This fundamental limitation necessitates a different use of springs to bypass the top speed of natural running.

We conceive an unconventional means of running, which could allow the human to maximize top running speed by supplying energy in the air instead of on the ground (Fig. 1). This may be achieved by augmenting the human with variable stiffness springs attached to the limbs. In the air, the limbs supply energy by simultaneously compressing and increasing the stiffness of the springs (Fig. 1A). Upon touchdown, the stiff springs redirect the vertical motion of the human instead of the legs, while the energy stored in the springs is released to increase the horizontal running speed (Fig. 1B). In the proposed augmented running, (i) the energy supplied by the limbs is no longer limited by the short ground contact time, (ii) the springs support the body instead of the limbs, and (iii) the springs mitigate collision energy losses like the wheel of a bicycle. Therefore, the proposed means of augmented running confers defining features of cycling, which may enable humans to go beyond the top speed of natural running (movie S1).

RESULTS

Building exoskeleton devices (*8*) and performing human-in-the-loop experimental exploration (*9*, *21*) are the mainstream and state-of-the-art approaches to develop novel human augmentation paradigms, although theoretical investigations may also be useful to uncover the benefits of previously unexplored augmentation methods (*22*). Simple spring-mass models (*18*, *19*) have been previously used to provide useful theoretical predictions of the biomechanics of natural running (*23*, *24*). These models use a point mass to represent the body and a spring to represent the biological limb, and assume symmetric ground contact while neglecting air resistance in natural running. Here, we use a similarly simple model (Fig. 1C) to explore the theoretical benefits of augmented running. In our model, the spring represents the augmentation device instead of the biological limb, we consider asymmetric ground contact motion, and we assume that air resistance is nonnegligible in high-speed running (*17*).

Our spring-mass model (Fig. 1C) discovers stable augmented running (fig. S2) and provides the following analytical predictions beyond the top speed of natural running (see Materials and Methods):

(i) The peak force F and the stiffness k of the spring on the ground increase nonlinearly with the running speed (c is a constant)

$$F \propto \sqrt{k} \propto \frac{1}{1 + cv^{-2}}$$

(ii) The ground contact time is inversely proportional to the running speed, while the time available to swing the leg approaches the step duration T at high speeds

$$\Delta t_g \propto v^{-1} \text{ and } \Delta t_s \approx T$$

According to these predictions, (i) surpassing the top speed of natural running requires a spring to provide force and stiffness beyond human limb capability and (ii) the time available for the legs to supply energy in the air approaches the continuous limit of

Center for Rehabilitation Engineering and Assistive Technology, Advanced Robotics and Control Laboratory, Vanderbilt University, 2301 Vanderbilt Place, Nashville, TN 37235, USA.
*Corresponding author. Email: david.braun@vanderbilt.edu

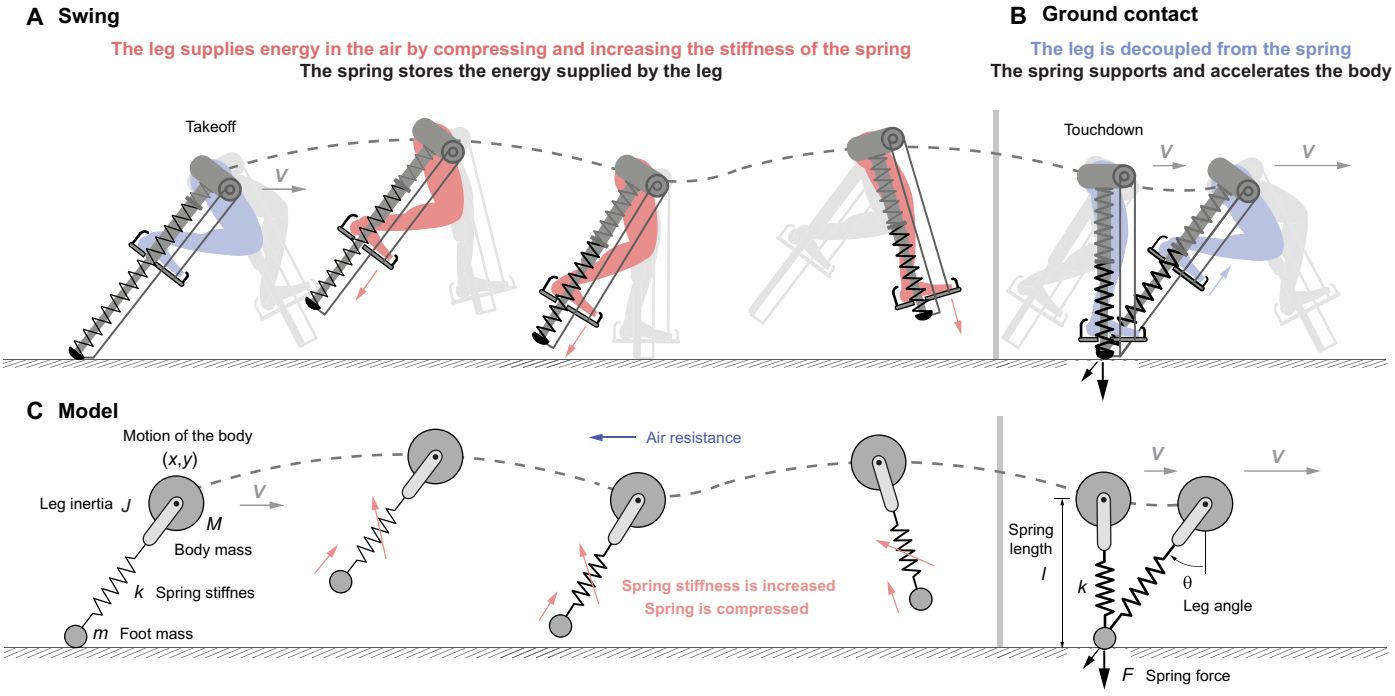

Fig. 1. Augmented running. The augmentation device is a robotic exoskeleton represented by a variable stiffness spring. (**A**) Swing. The leg is coupled to the spring. As the leg extends, the spring is compressed and the stiffness of the spring is increased. The latter can be achieved by a variable stiffness mechanism, which increases stiffness by decreasing the effective length of the spring [see (*28*, *30*–*32*), Materials and Methods, and movie S1]. The exoskeleton provides mechanical advantage to the human such that large leg extension, small leg force, and small leg stiffness provide small spring compression, large spring force, and large spring stiffness. (**B**) Ground contact. The leg is decoupled from the spring and the mechanism that changes stiffness is locked. As the leg flexes, the spring extends while the stiffness of the spring stays constant. (**C**) Spring-mass model of augmented running.

cycling. The model also predicts that the runner may supply energy during 96% of the step time ($T = \Delta t_g + \Delta t_s$) at the top running speed. If this were possible, the speed limit of running due to air resistance would be 97% of the air resistance limit in cycling 22.6 m/s. This prediction assumes the energy supply rate of 18 W/kg for the biological limb in running (*25*), which is slightly below the estimated energy supply rate of world-class sprint cyclists (*26*).

The theoretical top speed of augmented running is lower than the aforementioned air resistance limit and can be predicted by extending the model to account for the most substantial energy losses in addition to the biological limitation of the limb. Considering the collisional energy losses upon ground contact (*27*) due to the mass of the spring (Fig. 1C), the kinetic energy required to swing the stance leg with nonnegligible rotational inertia, and the limited stepping frequency of the current world record holder sprinter Usain Bolt (*1*), the model predicts 20.9 m/s. This speed is 2.4% below the current world record cycling speed (Fig. 2).

Figure 3 provides a detailed account of augmented running predicted by the model (solid lines) compared to the estimated and measured data from natural running and cycling (dashed lines) (fig. S7) (*1*, *2*, *17*). According to these predictions, the augmented running may reach the top speed of natural running $v^N_{max} \approx 12.3$ m/s in 10 steps and may require 150 steps to reach $v_{max} \approx 20.9$ m/s. At the top speed, the time available to supply energy in the air $\Delta t_s \approx 533$ ms is six times longer than the ground contact time in natural running $\Delta t^N_g \approx 90$ ms and 1.5 times longer than the swing time in natural running $\Delta t^N_s \approx 354$ ms, while the ground contact time in augmented running $\Delta t_g \approx 19.3$ ms is more than four times shorter than the ground contact time in natural running (Fig. 3B). On the ground, the spring exerts a maximum force of $F \approx 21$ kN, which is six times the maximum force exerted by the human $F^N \approx 3.6$ kN (Fig. 3C), while the stiffness of the spring $k \approx 234$ kN/m is 11 times the stiffness of a human leg at the top speed of natural running $k^N \approx 21$ kN/m (Fig. 3D). The physical requirements in augmented running are beyond the capability of a biological limb but may be achieved using a robotic variable stiffness spring exoskeleton.

DISCUSSION

Emerging human augmentation technologies (*22*, *28*, *29*) promote active variable stiffness springs, where the stiffness is adjusted using an actuator that requires external energy (*30*–*33*). In augmented running (Fig. 2), the variable stiffness spring is an energetically passive device where the stiffness of the spring is adjusted by the human, without using external energy. In addition, the variable stiffness spring enables the human to supply energy when the legs are in the air, which makes the energy supplied by the legs independent of the short ground contact time. In this way, the spring could enable the human to bypass the fundamental physical limitation of natural running (*6*), despite providing no external energy.

The energy supplied by the human per step is the product of the average energy supply rate of the limbs, and the time available to supply energy $E = \bar{E}\,\Delta t_E$. Assuming that the average energy rate of the limbs $\bar{E}$ is maximized by the human to achieve the top speed,

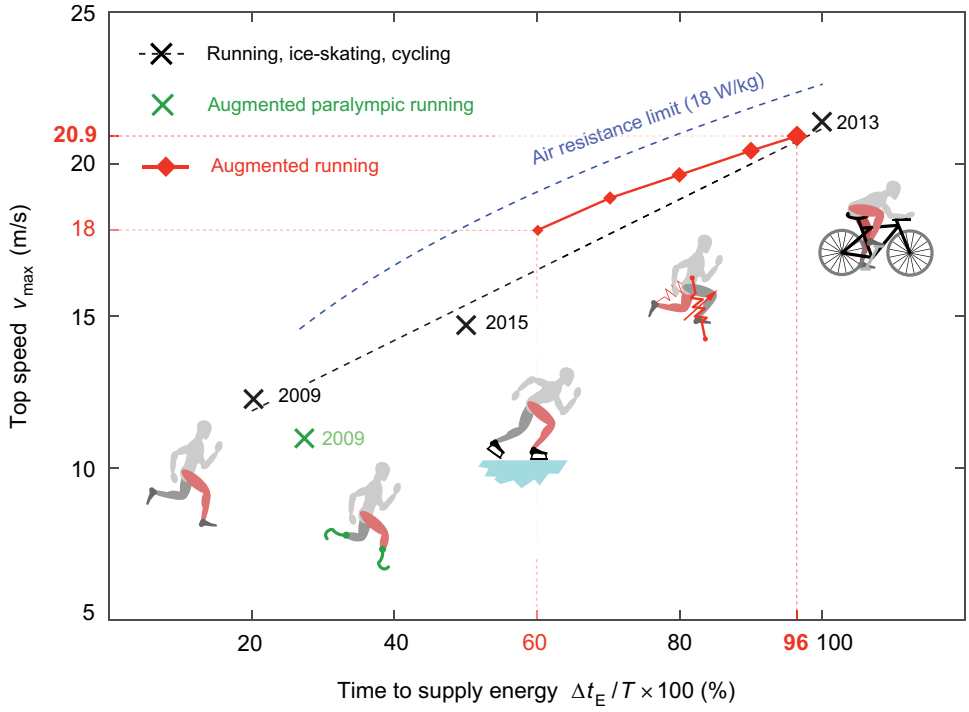

Fig. 2. Top speeds of human-powered locomotion. World records in natural running (12.3 m/s) (*1*), running with a spring blade prosthesis (11 m/s) (*13*), ice-skating (15 m/s) (*52*), and cycling (21.4 m/s) (fig. S7) (*2*) and the top speed predicted for augmented running (20.9 m/s). There is a linear empirical relation $v_{max} \propto \Delta t_E/T$ between the world record speeds and the relative time available for each leg to supply energy in running, ice-skating, and cycling. The air resistance limit is given by a cube-root relation $v_{max} \propto (\Delta t_E/T)^{1/3}$ (see Materials and Methods). This relation is calculated assuming that the energy supply rate of each leg is 18 W/kg (*25*), which is near to what has been measured for world-class cyclists (*26*).

the only way to provide more energy is to increase the time to supply energy

$$\frac{E}{E_{max}} = \frac{\Delta t_E}{T}$$

According to Fig. 3B, the proposed augmented running could theoretically enable the human to provide energy 96% of the total step time (black triangles), similar to what is analytically predicted by the spring-mass model (blue line). If that was possible, the time to supply energy in augmented running could be more than the 20% in natural running and 50% in ice-skating and would be close to the continuous limit of 100% in cycling (Fig. 2).

In addition to increasing the time available for the human to supply energy, the variable stiffness spring is used as a catapult to release energy faster than the energy supply rate of the biological limb. To make use of the catapult action, an energy-storing element, for example, tendon in animals (*16*) or spring in robots (*34*), is first preloaded in the air by an actuator, muscle, or motor, and then used to push against the ground faster than the actuator could alone do. While a typical catapult that uses a fixed stiffness spring may amplify both the power and the force of a limb, it could not change its stiffness as required to redirect vertical motion and accelerate horizontal motion of the human at different speeds (Fig. 3A) (*19*, *20*). Therefore, augmented running necessitates the use of a variable stiffness catapult (Fig. 3D).

To predict the top augmented running speed of 20.9 m/s (Figs. 2 and 3), we have assumed that (i) the human can supply energy during the entire swing phase, i.e., 96% of the step; (ii) the energy supply rate of a human, 18 W/kg per leg (*25*), is comparable to the energy supply rate of world-class cyclists (19 W/kg) (*26*); and (iii) the spring transfers all the energy supplied by the legs in the air to accelerate the forward motion of the body on the ground. If these assumptions are not met, then the amount of energy provided by the legs will be reduced and the top speed will be lower than 20.9 m/s. However, even if energy is supplied only 60% of the total step time, the reduced top speed of augmented running, 18 m/s, remains 50% above the current top speed of natural running (Fig. 2).

To reach the theoretical top speed of 20.9 m/s in Fig. 2, the spring should (i) store 930 J energy and (ii) weigh no more than 1.5 kg and (iii) the stiffness of the spring should reach one order of magnitude beyond the maximum stiffness of the leg in natural running (Fig. 3D). Variable stiffness springs may be designed with a wide stiffness range (*31*), and carbon fiber–reinforced polymers or air-springs have high energy capacity while being lightweight (*35*). However, state-of-the-art fixed stiffness running springs made from carbon fiber offer only about 150 J/kg (*36*), which is an order of magnitude less than what is required to reach the predicted top speed of augmented running. A novel high-energy density variable stiffness spring design will be required to realize high-speed augmented running.

Current running exoskeletons use fixed stiffness springs in parallel with the legs to support the body (*7*) but require the human to supply energy while pushing against the ground, as in natural running (*37*, *38*). The limitation of these exoskeletons, in reducing the metabolic energy cost of running, has been attributed to (i) the energy required to swing the legs with the added mass of the exoskeleton and (ii) the inefficient energy transfer between the human and the exoskeleton.

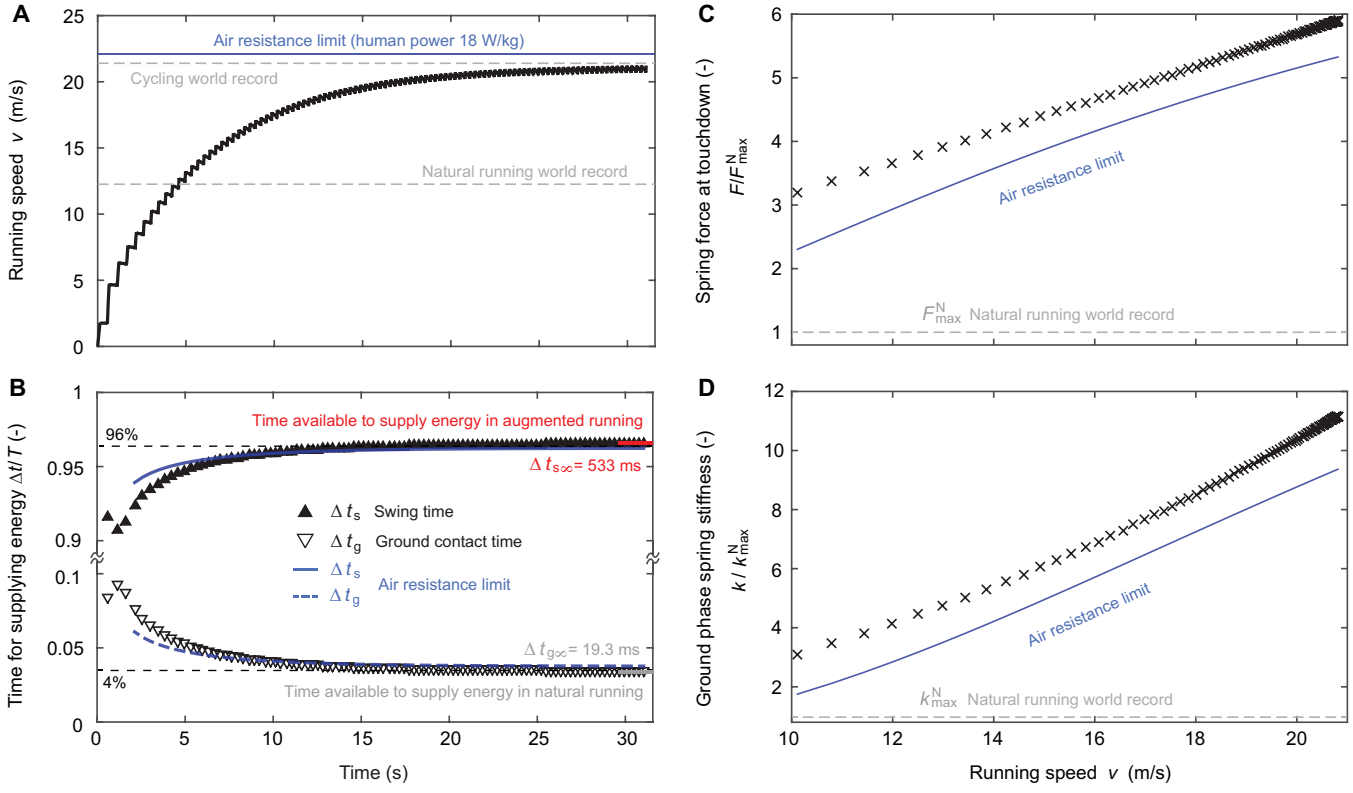

Fig. 3. Augmented running. (**A**) Running speed. (**B**) Swing and stance times. (**C**) Ground reaction force at touchdown. (**D**) Spring stiffness during ground contact. The top speed predicted by the model (20.9 m/s, black) is approximately 96% of the air resistance limit (21.9 m/s, blue). The average acceleration of the body is within safely tolerable accelerations (fig. S3). The parameters used to obtain these predictions are taken from the current world record holder sprinter Usain Bolt (table S1).

These findings suggested that engineering innovations are required to improve the performance of exoskeletons developed for human augmentation (*39*). However, even if we hypothesize an ideal massless exoskeleton and consider perfect energy transfer between the human and the exoskeleton, the air resistance speed limit of the human augmented with a fixed stiffness spring remains 65% of the air resistance speed limit in cycling (see Materials and Methods). This is because the human augmented with a fixed stiffness spring could supply energy no more than 30% of the total step time when pushing against the ground as in natural running, which is less than the 96% in the proposed augmented running or the 100% in cycling (Fig. 2, dashed blue line). A fixed stiffness spring in parallel with the legs is similar to a bicycle without pedals; it helps to support the body in the vertical direction but does not help to accelerate the body in the horizontal direction (*5*). The variable stiffness spring supports the body, but it also provides an equivalent pedaling mechanism as it enables the human to supply energy beyond what is possible in natural running.

Historical data (fig. S7) show that the world record average speed in the 100-m sprint has increased 6% in the past 70 years, while the world record average speed in the 500-m speed skating and 200-m track cycling have increased as much as 23% in the same time period. The relatively large increase in skating and cycling speeds has been attributed to engineering advances, as decades of technical innovations were required before clap skates (*40*) allow the human to go considerably beyond the world record running speed, and racing bicycles (*5*) allowed the human to double the world record running speed (fig. S7). The development of variable stiffness spring exoskeletons for high-speed augmented running could follow a similar path.

MATERIALS AND METHODS

In this section, we first present the variable stiffness spring-mass model of augmented running, which takes into account air resistance, collision losses, and the limited power of the biological limb. We use this model to numerically predict the top speed of the augmented running motion. Subsequently, we derive an approximate spring-mass model of running to analytically predict the relations between the running speed, spring stiffness, spring force, and the ground contact time in high-speed running. Next, we provide a stability analysis of the augmented running motion using both of the previously derived models. Last, we derive (i) the air resistance speed limit of augmented running where the human does work in the air, as in cycling, and (ii) the air resistance speed limit of augmented running where the human does work on the ground, as in natural running.

Spring-mass model of augmented running

The spring-mass model of augmented running is depicted in Fig. 1C and fig. S1. The differential equations governing the flight phase and ground contact phase motions are given by

$$(M + 2m)\ddot{x} = -F_{\text{air}},\ \ddot{y} = -g \quad (1)$$

and

$$(M + m)(\ddot{l} - l\dot{\theta}^2) = -(M + m)g\cos\theta + k(l_0 - l) - F_{\text{air}}\sin\theta \quad (2)$$

$$(J + (M + m)l^2)\ddot{\theta} + 2(M + m)\dot{l}l\dot{\theta} = (M + m)gl\sin\theta - F_{\text{air}}l\cos\theta \quad (3)$$

where (x, y) are the Cartesian coordinates of the body, l is the length of the spring, θ is the rotation angle of the leg and the spring, M is the total mass of the human, m is the mass of the spring attached to one of the legs, J is the rotational inertia of the leg, F_{air} is the force due to air resistance, k is the stiffness of the spring during the ground contact phase, F is the force exerted by the spring against the ground, and g is the gravitational acceleration. We assume that the spring mass is concentrated at the foot, which is the worst-case mass distribution of the spring.

Furthermore, we assume that air resistance is proportional to the squared running speed (*17*)

$$F_{air} = c_{air}\dot{x}^2 \tag{4}$$

where c_{air} is an empirical constant. All parameters in Eqs. 1 to 4 are given in table S1.

The transition between the flight phase and the ground contact phase occurs at touchdown

$$y_{td} = l_{td}\cos\theta_{td}$$

where l_{td} represents the length of the spring at touchdown, while θ_{td} is the touchdown angle. We assume ideally plastic collision between the foot and the ground; therefore, based on momentum conservation, the velocity of the body changes according to the following relations

$$\dot{l}_{td}^{+} = \dot{x}_{td}^{-}\sin\theta_{td} + \dot{y}_{td}^{-}\cos\theta_{td},$$
$$\dot{\theta}_{td}^{+} = \dot{\theta}_{td}^{-} - \frac{(M+m)\,l_{td}^2}{J+(M+m)\,l_{td}^2}\left(\dot{\theta}_{td}^{-} + \dot{y}_{td}^{-}\frac{\sin\theta_{td}}{l_{td}} - \dot{x}_{td}^{-}\frac{\cos\theta_{td}}{l_{td}}\right)$$

where $(\cdot)^-$ and $(\cdot)^+$ denote the pre-impact and post-impact velocities, respectively. We assume that the human does not supply energy to increase the angular velocity of the leg in swing; the angular velocity at touchdown $\dot{\theta}_{td}^{-}$ in the current step is the same as the angular velocity upon takeoff in the previous step. Because the mass of the spring is concentrated at the foot, the impact of the leg with the ground gives the highest energy loss at touchdown (*27*).

The transition between ground contact and flight occurs at the maximum length of the spring due to a hard stop (fig. S1) that prevents extension of the spring

$$l_{to} = l_0$$

where l_{to} is the length of the spring at takeoff. When the hard stop is reached, a plastic collision takes place and the velocity of the body changes due to momentum conservation

$$\dot{x}_{to}^{+} = \left(1 - \frac{m}{M+2m}\sin\theta_{to}^{\,2}\right)\dot{x}_{to}^{-} - \frac{1}{2}\frac{m}{M+2m}\dot{y}_{to}^{-}\sin 2\theta_{to},$$
$$\dot{y}_{to}^{+} = \left(1 - \frac{m}{M+2m}\cos\theta_{to}^{\,2}\right)\dot{y}_{to}^{-} - \frac{1}{2}\frac{m}{M+2m}\dot{x}_{to}^{-}\sin 2\theta_{to}$$

The spring-mass model of augmented running accounts for air resistance, the rotational moment of inertia of the leg, the mass of the spring concentrated at the foot, and the collisional energy loses at touchdown and takeoff. These features extend prior spring-mass models of natural running (*18*, *19*, *24*, *41*–*43*).

Touchdown angle of the human

We allow asymmetric ground contact with vertical and forward leaning leg touchdown (Fig. 1B)

$$\theta_{td} \neq -\theta_{to},\ \theta_{td} \geq 0 \tag{5}$$

Forward leaning touchdown ($\theta_{td} > 0$) is required in the initial steps when the motion resembles the start of a sprint (*44*). Forward leaning or vertical leg touchdown can be used to avoid the braking phase ($\theta_{td} < 0$) in which the spring impedes the running motion. Last, a vertical leg touchdown ($\theta_{td} = 0$ Fig. 1B) minimizes the stiffness of the spring to redirect vertical motion upon landing and could allow the human to maximize the forward acceleration to reach higher speeds (*25*). Therefore, we assume that a vertical leg touchdown is desired in high-speed augmented running

$$\theta_{td} = 0 \tag{6}$$

Energy supplied by the human

The extension of the leg in augmented running resembles the pedaling of a bicycle (Fig. 1, A and B). Therefore, we assume that the average energy supply rate of one leg in augmented running is (*25*)

$$\frac{\dot{\bar{E}}_{leg}}{M} \approx 18\ \mathrm{W/kg} \tag{7}$$

which is comparable to the average energy supply rate in world-class sprint cycling (19 W/kg) (*26*). Relation 7 implies that the energy supplied by the legs during the swing phase in augmented running is three times the energy supplied by the legs during the ground contact phase of natural running

$$E_{leg} \approx \dot{\bar{E}}_{leg}\Delta t_{s\infty} \approx 3E_{leg}^{N} = 3\,\bar{F}^{N}\Delta l_s^{N} = \frac{3}{2}F_{max}^{N}\Delta l_s^{N} \tag{8}$$

where $\Delta t_{s\infty}$ is the swing time at the top speed of augmented running, Δl_s^N is the distance moved by the leg, and $\bar{F}^N$ is the average ground contact force in natural running (table S1) (*13*, *45*). Similar to cycling (*26*), the legs could supply this energy using longer and slower extension compared to natural running, because the swing time in augmented running ($\Delta t_s \geq \Delta t_{s\infty} = 533$ ms) is more than six times longer than the ground contact time in natural running ($\Delta t_g^N = 90$ ms) (see Fig. 3B).

Variable stiffness spring

During swing (Fig. 1A), the leg extends to compress the spring and to simultaneously increase the stiffness of the spring. The stiffness of the spring is increased by coupling the leg to a variable stiffness mechanism, which decreases the effective length of the spring (*28*, *30*, *32*, *33*). As a result, the force of the spring and the energy stored by the spring increase

$$F = k(\Delta l_{leg})\,\Delta l(\Delta l_{leg}) + \mathcal{O}(\Delta l^3) \text{ and } E_{spr} = \int_0^{\Delta l_{max}} F d\Delta l$$

One of the simplest examples of such mechanism is a helical spring with changeable active length used in parallel with a fixed stiffness spring. The stiffness of that mechanism is given by

$$k(\Delta l_{leg}) = k_0 + (k_{max} - k_0)\frac{L_{min}}{L(\Delta l_{leg})}$$

where the active length of the spring is set by the motion of the leg $L(\Delta l_{leg}) \in [L_{min}, L_{max}]$ and $k_0 = (k_{min}L_{max} - k_{max}L_{min})/(L_{max} - L_{min})$. Movie S1 shows the augmented running motion driven by one such spring.

During ground contact (Fig. 1B), the spring is decoupled from the leg, while the variable stiffness mechanism is locked, rendering the stiffness constant

$$\forall \Delta l_{leg}: F = k\Delta l + \mathcal{O}(\Delta l^3) \tag{9}$$

Decoupling the spring from the leg and locking the variable stiffness mechanism can be performed with negligible energy cost via a clutch, because these operations neither supply energy for the running motion nor add energy to the spring (*22*). This is similar to changing gears on a bicycle, which can be performed with an effortless finger movement (*46*) because changing gears does not supply energy to move the bicycle.

Augmented running

The work cycle of the spring in augmented running is as follows. Upon takeoff (Fig. 1A), the leg extends to supply energy (Eq. 8) and the spring stores that energy

$$E_{spr} = E_{leg} \tag{10}$$

On the ground (Fig. 1B), the energy stored by the spring is released to increase the horizontal kinetic energy of the body

$$E_{kx,to} - E_{kx,td} = E_{spr} - E_{loss} \tag{11}$$

where $E_{kx,to}$ and $E_{kx,td}$ denote the kinetic energy of the horizontal motion of the body from touchdown to takeoff, while E_{loss} is the sum of the collisional loss at touchdown, the energy loss at takeoff, the energy loss due to air resistance, and the energy required to rotate the stance leg augmented with the spring.

Numerical prediction

Using the model Eqs. 1 to 3, and the parameters in table S1, we predicted the motion of the spring-mass system. The model was started from rest, tilted forward with one of the legs touching the ground to resemble the starting position of a runner in a 100-m sprint (fig. S6A)

$$x(0) = x_0,\ y(0) = y_0,\ \dot{x}(0) = 0,\ \dot{y}(0) = 0$$

In the first step (fig. S6B), the force is provided by one of the legs. This force is set large enough to ensure that the leg can swing forward before the subsequent touchdown $\Delta t_s/2 + \Delta t_g/2 = T/2 \geq f_{max}^{-1}$ where f_{max} is the maximum stepping frequency defined by

$$f \leq f_{max} = f_{max}^{N}\left(\frac{J}{J + ml_0^2}\right)^{\frac{1}{2}} \tag{12}$$

After the first step (fig. S6, B and C), the force on the ground is provided by the spring.

In the swing phase (Fig. 1A), we use the average energy rate of the leg in natural running $\bar{\dot{E}}_{leg}$ (Eq. 8) and assume that the energy provided by the human at every step is limited by the energy the leg could provide at the top speed

$$E_{spr} = \bar{\dot{E}}_{leg}\Delta t_{s\infty} \leq \bar{\dot{E}}_{leg}\Delta t_s$$

This is the most conservative estimate for the energy supplied in each step, as the swing time is the shortest at the top speed $\Delta t_{s\infty} \leq \Delta t_s$.

We assume that the spring is linear during ground contact $F = k\Delta l$ (Eq. 9) such that the stiffness of the spring k governing the ground contact phase motion is given by

$$E_{spr} = \frac{1}{2}k\Delta l_{td}^2 \Rightarrow k = \frac{2E_{spr}}{\Delta l_{td}^2} \tag{13}$$

while the compression of the spring Δl_{td} is defined by

$$\mathcal{F}(\Delta l_{td}, \dot{x}_{td}) = E_{ky,td} - E_{ky,to} + Mg(y_{td} - y_{to}) = 0 \tag{14}$$

The latter equation is derived by subtracting the equation that governs the ground contact phase motion of augmented running (Eq. 11) from the energy balance equation $E_{k,to} + Mgy_{to} = E_{k,td} + Mgy_{td} + E_{spr} - E_{loss}$.

We solve Eq. 14 to find Δl_{td} by first assuming Δl_{td}, then solving the flight phase equations of motion (Eq. 1) analytically until $y_{td} = l_0 - \Delta l_{td}$ to find $E_{ky,td}$ at touchdown, and finally numerically simulating the ground phase motion (Eqs. 2 and 3) to find y_{to} and $E_{ky,to}$ at takeoff. We find Δl_{td} that satisfies Eq. 14 using the bisection method. In particular, first we assume a vertical leg touchdown $\theta_{td} = 0$ (Eq. 6) and find Δl_{td} by solving Eq. 14. If no feasible spring compression $\frac{1}{2}l_0 \leq \Delta l_{td} \leq l_0$ exists with vertical touchdown, then the touchdown angle is increased $\theta_{td} > 0$ (Eq. 5) until a feasible spring compression $\frac{1}{2}l_0 \leq \Delta l_{td} \leq l_0$ is found. In our simulations, vertical leg touchdown was feasible for high-speed augmented running, including the top speed of natural human running (fig. S6C). On the other hand, the legs had to be tilted forward during the starting steps to ensure feasible leg compression at low speeds (fig. S6B).

Spring-mass model of high-speed augmented running

Assuming that (i) the effect of air resistance is negligible during the short ground contact phase compared to the effect of air resistance during the substantially longer aerial phase of running, (ii) collisional energy losses are negligible compared to the kinetic energy at touchdown, (iii) the change in kinetic energy of the stance leg is negligible compared to the change of the translational kinetic energy of the body, and (iv) the mass of the spring is negligible compared to the mass of the body, the nonlinear model (Eqs. 2 and 3) reduces to the spring-mass model of natural running (*18*, *19*, *24*, *41*, *42*)

$$M\Delta\ddot{x} = F_x(\Delta x, y) = k\left(\frac{l_0\Delta x}{\sqrt{\Delta x^2 + y^2}} - \Delta x\right) \tag{15}$$

$$M\ddot{y} = F_y(\Delta x, y) = k\left(\frac{l_0 y}{\sqrt{\Delta x^2 + y^2}} - y\right) - Mg \tag{16}$$

where Δx is the horizontal distance between the body and the foot during ground contact.

Equations 15 and 16 have no known analytical solution, and nonlinear approximations have been previously used to facilitate in-depth analysis of these equations when considering natural running (*42*). In what follows, we present a nonlinear approximation of Eqs. 15 and 16 to investigate the essential physics of high-speed augmented running.

First, we assume that the vertical position of the body is approximately constant in high-speed running

$$y(t) \approx y_{td} = \text{const} \tag{17}$$

Under this assumption, the forces in Eqs. 15 and 16 simplify to

$$F_x(\Delta x, y) = F_x(\Delta x, y_{td}) + \mathcal{O}(y - y_{td}) \tag{18}$$

$$F_y(\Delta x, y) = F_y(\Delta x, y_{td}) + \mathcal{O}(y - y_{td}) \tag{19}$$

Next, we apply a first-order Fourier series approximation of Eqs. 18 and 19, subject to three conditions

(i) The condition of vertical leg touchdown (Eq. 6)

$$\Delta x(0) = 0 \tag{20}$$

(ii) The conditions at touchdown and takeoff

$$\begin{aligned} F_x(0, y_{td}) &= 0, \quad & F_y(0, y_{td}) &= k(l_0 - y_{td}) - Mg, \\ F_x(\Delta x_{max}, y_{to}) &= 0, \quad & F_y(\Delta x_{max}, y_{to}) &= -Mg \end{aligned} \tag{21}$$

(iii) The energy balance during ground contact

$$E_{kx,to} - E_{kx,td} = \int_0^{\Delta x_{max}} F_x(\Delta x, y_{td})\, d\Delta x = E_{spr} \tag{22}$$

The last condition is obtained from Eq. 11 by assuming that the energy loss during ground contact is negligible. This assumption is consistent with Eqs. 15 and 16.

Using the first-order Fourier series approximation of $F_x(\Delta x, y_{td})$ and $F_y(\Delta x, y_{td})$, together with Eqs. 20 to 22, we obtain an approximate spring-mass model of augmented running

$$M\Delta\ddot{x} = \hat{F}_x(\Delta x) \approx \frac{\pi E_{spr}}{2\Delta x_{max}} \sin\left(\pi \frac{\Delta x}{\Delta x_{max}}\right) \tag{23}$$

$$M\ddot{y} = \hat{F}_y(\Delta x) \approx k(l_0 - y_{td}) \cos\left(\frac{\pi}{2} \frac{\Delta x}{\Delta x_{max}}\right) - Mg \tag{24}$$

According to fig. S4, the relative error between the forces in Eqs. 18, 19, 23, and 24 is no more than 10% beyond the top speed of natural running. Next, we use the approximate model (Eqs. 23 and 24) to derive scaling laws for high-speed augmented running.

Spring stiffness and spring compression

The ground phase stiffness is given by Eq. 13

$$k = \frac{2E_{spr}}{\Delta l_{td}^2} \tag{25}$$

where Eq. 14 defines the spring compression at touchdown Δl_{td}. Using Eq. 17, Eq. 14 reduces to

$$E_{ky,td} - E_{ky,to} \approx \frac{1}{2} M\dot{y}(0)^2 - \frac{1}{2} M\dot{y}(\Delta x_{max})^2 = 0 \tag{26}$$

To derive the analytical expression of Eq. 26 as a function of Δl_{td}, we will derive $\dot{y}(\Delta x)$ using Eqs. 23 and 24. First, we integrate Eq. 23 to obtain the relation between the horizontal velocity and the horizontal position

$$\Delta\dot{x}(\Delta x) = \dot{x}(\Delta x) \approx \dot{x}_{td} \left[1 + \frac{2E_{spr}}{M\dot{x}_{td}^2} \sin\left(\frac{\pi}{2} \frac{\Delta x}{\Delta x_{max}}\right)^2\right]^{\frac{1}{2}} \tag{27}$$

Next, we use Eq. 27 to integrate Eq. 24 and obtain the relation between the vertical velocity and the horizontal position

$$\dot{y}(\Delta x_{max}) \approx \dot{y}_{td} + \frac{2^{\frac{1}{2}} k \Delta l_{td} \Delta x_{max}}{\pi M^{\frac{1}{2}} E_{spr}^{\frac{1}{2}}} \sinh^{-1}\left[\left(\frac{2E_{spr}}{M\dot{x}_{td}^2}\right)^{\frac{1}{2}}\right] - \frac{2^{\frac{1}{2}} M^{\frac{1}{2}} g \Delta x_{max}}{\pi E_{spr}^{\frac{1}{2}}} \text{sn}^{-1}\left[1 \middle| -\frac{2E_{spr}}{M\dot{x}_{td}^2}\right] \tag{28}$$

where sn(* | *) is the Jacobi elliptic sine function

$$\Delta x_{max} \approx (2 l_0 \Delta l_{td} - \Delta l_{td}^2)^{\frac{1}{2}} \tag{29}$$

is the horizontal position of the center of mass with respect to the foot at takeoff

$$\dot{y}_{td}^2 = \frac{2E_y}{M} - 2g(l_0 - \Delta l_{td}) \tag{30}$$

is the vertical velocity at touchdown, while E_y is the total energy of the vertical motion. Using Eqs. 25 to 30, we obtain the approximate analytical expression of Eq. 26

$$\mathcal{F}(\Delta l_{td}, \dot{x}_{td}) = \left(\frac{2E_y}{M} - 2g(l_0 - \Delta l_{td})\right)^{\frac{1}{2}} - \frac{(2E_{spr})^{\frac{1}{2}} (2l_0 - \Delta l_{td})^{\frac{1}{2}}}{\pi (M \Delta l_{td})^{\frac{1}{2}}} \sinh^{-1}\left[\left(\frac{2E_{spr}}{M\dot{x}_{td}^2}\right)^{\frac{1}{2}}\right] + \frac{g \Delta l_{td}^{\frac{1}{2}} (2l_0 - \Delta l_{td})^{\frac{1}{2}}}{\dot{x}_{td}} \text{sn}^{-1}\left[1 \middle| -\frac{2E_{spr}}{M\dot{x}_{td}^2}\right] = 0 \tag{31}$$

The approximate spring compression at touchdown $\Delta l_{td} = \Delta l_{td}(\dot{x}_{td})$ is the solution of Eq. 31.

Scaling laws

We derived closed-form relations between (i) the stiffness of the spring during ground contact k, (ii) the force of the spring at touchdown F, (iii) the ground contact time Δt_g, and the forward speed at touchdown $v = \dot{x}_{td}$.

We assume that the horizontal kinetic energy of the body is much greater than the energy stored in the spring in high-speed running

$$e = \frac{2E_{spr}}{Mv^2} \approx e_{min} = \frac{2E_{spr}}{Mv_{max}^2} \ll 1 \tag{32}$$

Using Eq. 32, we transform Eq. 31 into

$$\left(\frac{\Delta l_{td}}{l_0}\right)^2 - (b_0 + b_1 e)\left(\frac{\Delta l_{td}}{l_0}\right) - c_1 e = \mathcal{O}\left(e \frac{\Delta l_{td}^3}{l_0^3}\right) \tag{33}$$

where b_0, b_1, and c_1 are constants dependent on the top speed. We assume that the third-order term in Eq. 33 is negligible because the deformation of the spring Δl_{td} is smaller than the length of the leg

$$\frac{1}{2} l_0 \le y_{td} = l_0 - \Delta l_{td} \le l_0 \Rightarrow 0 \le \frac{\Delta l_{td}}{l_0} \le \frac{1}{2} \tag{34}$$

and because Δl_{td} reduces as the running speed increases (fig. S6). Consequently, Eq. 33 can be analytically solved to predict the largest deformation of the spring at touchdown

$$\frac{\Delta l_{td}(e)}{l_0} \approx \frac{(b_0 + b_1 e) + \sqrt{(b_0 + b_1 e)^2 + 4 c_1 e}}{2} \tag{35}$$

Substituting Eq. 35 into Eq. 25, we obtain the lowest stiffness that satisfies Eq. 31 and the maximum ground contact time when running at speed $v = \dot{x}_{td}$. Near to saturation $e \approx e_{min}$, the compression of the spring obeys the following approximate relation

$$\frac{\Delta l_{td}(e)}{l_0} \approx \frac{\Delta l_{td}(e_{min})}{l_0} + \frac{d}{de}\left(\frac{\Delta l_{td}(e)}{l_0}\right)\Big|_{e_{min}} (e - e_{min}) \tag{36}$$

Using Eqs. 35 and 36, we obtain the scaling laws for high-speed augmented running

(i) The stiffness of the spring (Eq. 25) is given by

$$\sqrt{k} \propto \frac{\Delta l_{td}(e_{min})}{\Delta l_{td}(e)} \propto \frac{1}{1 + c v^{-2}} \tag{37}$$

where $c = v_{max}^2 \alpha (1 - \alpha)^{-1}$ and

$$\alpha = e_{min}\left(\frac{\Delta l_{td}(e_{min})}{l_0}\right)^{-1} \frac{d}{de}\left(\frac{\Delta l_{td}(e)}{l_0}\right)\Big|_{e_{min}} = \frac{2E_{spr}}{M v_{max}^2}\left[\frac{\Delta l_{td}}{l_0}\left(\frac{2E_{spr}}{M v_{max}^2}\right)\right]^{-1} \frac{d}{de}\left(\frac{\Delta l_{td}(e)}{l_0}\right)\Big|_{\frac{2E_{spr}}{M v_{max}^2}}$$

(ii) The force of the spring at touchdown $F = k\Delta l_{td}$ is given by

$$F \propto \frac{\Delta l_{td}(e_{min})}{\Delta l_{td}(e)} \propto \frac{1}{1 + c v^{-2}} \tag{38}$$

(iii) The ground contact time is given by

$$\Delta t_g \propto \left(\frac{e}{e_{min}}\right)^{\frac{1}{2}} \propto v^{-1} \tag{39}$$

To derive Eq. 39, we computed the ground contact time by integrating Eq. 27

$$\Delta t_g = \frac{2^{\frac{1}{2}} M^{\frac{1}{2}} \Delta x_{max} e^{\frac{1}{2}} \mathrm{sn}^{-1}(1|-e)}{\pi E_{spr}^{\frac{1}{2}}} \tag{40}$$

and assuming Eqs. 29, 32, 36, and 40, together with $e \ll 1$ (Eq. 32), such that $\mathrm{sn}^{-1}(1|-e) \approx \pi/2$.

Stability of the augmented running motion

The stability of the augmented running motion is characterized by a one-dimensional Poincaré return map (*15*, *47*) of the forward velocity at subsequent touchdowns $v_n = \dot{x}_{td,n}$ and $v_{n+1} = \dot{x}_{td,n+1}$

$$v_{n+1} = \mathcal{P}(v_n) \tag{41}$$

The existence of a fixed-point $v_{max} = \mathcal{P}(v_{max})$ implies the possibility of augmented running. The stability of the fixed point is characterized by the linear approximation of Eq. 41

$$(v_{n+1} - v_{max}) = \underbrace{\frac{\partial \mathcal{P}}{\partial v}\Big|_{v=v_{max}}}_{\lambda} (v_n - v_{max}) \tag{42}$$

which implies locally asymptotic stability if the magnitude of the eigenvalue is less than unity, $|\lambda| < 1$. Local stability of the fixed point implies local orbital stability of augmented running (*15*, *47*).

For the simplified spring-mass model, the composition of the swing and ground contact phase maps provides the relation between the vertical position and the horizontal velocity at subsequent touchdowns

$$\mathcal{P}_{sg} = \mathcal{P}_s \circ \mathcal{P}_g : (y_{td,n}, v_n) \rightarrow (y_{td,n+1}, v_{n+1}) \tag{43}$$

We reduced this two-dimensional map to a one-dimensional map using the analytical relation between the spring compression and the horizontal velocity at touchdowns $\mathcal{F}(\Delta l_{td}, v) = \mathcal{F}(l_0 - y_{td}, v) = 0$ (Eq. 31)

$$\mathcal{P} = \mathcal{P}_{sg}\big|_{\mathcal{F}(l_0 - y_{td,n}, v_n) = \mathcal{F}(l_0 - y_{td,n+1}, v_{n+1}) = 0} : v_n \rightarrow v_{n+1}$$

This one-dimensional map is represented by the following equation

$$\mathcal{G}(v_n, v_{n+1}) = \mathcal{G}(v_{max}, v_{max}) + \frac{\partial \mathcal{G}}{\partial v_n}\Big|_{v_n = v_{n+1} = v_{max}} (v_n - v_{max}) + \frac{\partial \mathcal{G}}{\partial v_{n+1}}\Big|_{v_n = v_{n+1} = v_{max}} (v_{n+1} - v_{max}) + \mathcal{O}\left[(v_n - v_{max})^2, (v_{n+1} - v_{max})^2\right] = 0$$

Using this equation, we define

$$\lambda = -\frac{\frac{\partial \mathcal{G}}{\partial v_n}\Big|_{v_n = v_{n+1} = v_{max}}}{\frac{\partial \mathcal{G}}{\partial v_{n+1}}\Big|_{v_n = v_{n+1} = v_{max}}}$$

Figure S5 summarizes the result of our stability analysis. The figure shows the set of feasible perturbations that would lead to orbitally stable augmented running, i.e., $|\lambda| < 1$.

Air resistance limit of the top speed in augmented running

The upper limit of the top running speed occurs when the average energy supply rate of the human equals the average rate of energy dissipation due to air resistance

$$\dot{\bar{E}}_{hum} = c_{air} v_{max}^3 \tag{44}$$

The average energy supply rate of the human is

$$\dot{\bar{E}}_{hum} = 2\dot{\bar{E}}_{leg}\frac{\Delta t_E}{T} \tag{45}$$

where $\dot{\bar{E}}_{leg} = E_{leg}/\Delta t_s$ is the average energy supply rate of one leg, while Δt_E is the time used by the leg to provide energy during the total step time T. According to Eqs. 44 and 45, the air resistance limit of the top speed of human-powered motion depends on the time available for the legs to supply energy (Fig. 2, dashed blue line)

$$v_{max} = \left(\frac{2\dot{\bar{E}}_{leg}}{c_{air}}\right)^{\frac{1}{3}} \left(\frac{\Delta t_E}{T}\right)^{\frac{1}{3}} \tag{46}$$

The time available for the legs to supply energy in augmented running is the time to swing the leg

$$\frac{\Delta t_E}{T} = \frac{\Delta t_s}{T} = \frac{T - \Delta t_g}{T} = 1 - \frac{1}{2} f \Delta t_g \tag{47}$$

where f denotes the stepping frequency. The ground contact time is inversely proportional to the forward speed and is upper bounded by

$$\Delta t_g \approx \frac{x_{to} - x_{td}}{v_{max}} \leq \frac{\Delta x_{max}}{v_{max}} \leq \frac{\sqrt{3}}{2}\frac{l_0}{v_{max}} \quad (48)$$

because Eqs. 5 and 34 imply

$$0 \leq \Delta x_{max}^2 \leq l_0^2 - y_{min}^2 \Rightarrow 0 \leq \frac{\Delta x_{max}}{l_0} \leq \frac{\sqrt{3}}{2}$$

Consequently, Eqs. 47 and 48 lead to

$$\frac{\Delta t_E}{T} \geq 1 - \frac{\sqrt{3}}{4}\frac{l_0 f}{v_{max}} \quad (49)$$

According to Eqs. 44, 45, and 49, the air resistance limit of augmented running can be approximated by the solution of the following equation

$$2\dot{\bar{E}}_{leg}\left(1 - \frac{\sqrt{3}}{4}\frac{l_0 f}{v_{max}}\right) = c_{air} v_{max}^3 \quad (50)$$

The approximate solution of Eq. 50 is given by

$$v_{max}^{run} \approx \left(\frac{2\dot{\bar{E}}_{leg}}{c_{air}}\right)^{\frac{1}{3}} - \frac{\sqrt{3}}{12} l_0 f \quad (51)$$

The difference between Eq. 51 and the exact solution of Eq. 50 is 0.1% for the parameters in table S1. Following the same derivation, the air resistance limit in cycling is given by

$$v_{max}^{cyc} \approx \left(\frac{\dot{\bar{E}}_{leg}}{\frac{1}{2}c_{air}}\right)^{\frac{1}{3}} \quad (52)$$

where we assume that the air resistance coefficient in cycling is approximately half the air resistance coefficient in running (*48*), and the legs only supply energy during extension and do not supply energy during the flexion phase of pedaling (*49*). On the basis of Eqs. 51 and 52, we conclude that the air resistance limit of the top speed in augmented running is near to the air resistance limit of the top speed in cycling

$$\frac{v_{max}^{run}}{v_{max}^{cyc}} \approx 1 - \frac{\sqrt{3}}{12}\left(\frac{l_0 f_{max}^N}{v_{max}^{cyc}}\right)\left(\frac{f}{f_{max}^N}\right) \geq 1 - \frac{\sqrt{3}}{12}\left(\frac{l_0 f_{max}^N}{v_{max}^{cyc}}\right) \approx 0.97 \quad (53)$$

Last, we derive the air resistance limit of augmented running, assuming that the human supplies energy on the ground as in natural running, while the legs are augmented with fixed stiffness springs. In that case, the energy for the running motion is supplied on the ground, and therefore, the time available for the legs to supply energy is the ground contact time. To obtain the upper bound of the ground contact time, we permit running with negative touchdown angles, without assuming that such running technique would impede the motion of the runner. This assumption doubles the maximum distance moved by the body during the ground contact phase of the running motion and consequently doubles the ground contact time compared to running augmented with the proposed variable stiffness spring

$$\frac{\Delta t_E}{T} = \frac{\Delta t_g}{T} = \frac{1}{2} f \Delta t_g = \frac{1}{2} f \frac{2\Delta x}{v_{max}} \leq \frac{\sqrt{3}}{2}\frac{l_0 f}{v_{max}} \quad (54)$$

According to Eqs. 46 and 54, the air resistance limit of natural running augmented with a fixed stiffness spring is given by

$$v_{max\,FS}^{run} = \left(\frac{\sqrt{3}}{2} l_0 f\right)^{\frac{1}{4}}\left(\frac{2\dot{\bar{E}}_{leg}}{c_{air}}\right)^{\frac{1}{4}} \quad (55)$$

On the basis of Eqs. 52 and 55, we conclude that the air resistance limit of the top speed when the human does work on the ground cannot exceed 65% of the air resistance limit in cycling

$$\frac{v_{max\,FS}^{run}}{v_{max}^{cyc}} = \left(\frac{\sqrt{3}}{2}\frac{l_0 f_{max}^N}{v_{max}^{cyc}}\right)^{\frac{1}{4}}\left(\frac{f}{f_{max}^N}\right)^{\frac{1}{4}} \leq \left(\frac{\sqrt{3}}{2}\frac{l_0 f_{max}^N}{v_{max}^{cyc}}\right)^{\frac{1}{4}} \approx 0.65 \quad (56)$$

The reduced air resistance limit (Eq. 56) compared to the air resistance limit of the proposed augmented running (Eq. 53) is because the maximal duration for the legs to supply energy on the ground is less than 30% of the total step time $\Delta t_E/T \leq 0.3$ (Eq. 54) compared to the more than 96%, $\Delta t_E/T \geq 0.96$ (Eq. 49), in the proposed augmented running.

SUPPLEMENTARY MATERIALS

Supplementary material for this article is available at http://advances.sciencemag.org/cgi/content/full/6/13/eaay1950/DC1

Fig. S1. Spring-mass model of augmented running.
Fig. S2. Stable augmented running.
Fig. S3. Acceleration and ground contact time.
Fig. S4. Approximate spring force.
Fig. S5. Stability of augmented running.
Fig. S6. Motion of the body in augmented running.
Fig. S7. Average world record speed.
Table S1. Estimated physical parameters of the 100-m world record holder sprinter Usain Bolt.
Movie S1. Augmented running.
References (*50*–*53*)

REFERENCES AND NOTES

1. M. J. D. Taylor, R. Beneke, Spring mass characteristics of the fastest men on Earth. *Int. J. Sports Med.* **33**, 667–670 (2012).
2. UCI Track Cycling World Cup, Men's 200 m qualifying (2013). Accessed on 23 August 2019; https://www.uci.org/docs/default-source/about--discipline/about-track-cycling/men-elite-world-records.pdf?sfvrsn=244fc916_28.
3. A. Ruina, J. E. A. Bertram, M. Srinivasan, A collisional model of the energetic cost of support work qualitatively explains leg sequencing in walking and galloping, pseudo-elastic leg behavior in running and the walk-to-run transition. *J. Theor. Biol.* **237**, 170–192 (2005).
4. R. Kram, C. R. Taylor, Energetics of running: A new perspective. *Nature* **346**, 265–267 (1990).
5. A. E. Minetti, J. Pinkerton, P. Zamparo, From bipedalism to bicyclism: Evolution in energetics and biomechanics of historic bicycles. *Proc. R. Soc. Lond. B* **268**, 1351–1360 (2001).
6. P. G. Weyand, R. F. Sandell, D. N. Prime, M. W. Bundle, The biological limits to running speed are imposed from the ground up. *J. Appl. Physiol.* **108**, 950–961 (2010).
7. N. Yagn, Apparatus for facilitating walking, running, and jumping, U.S. Patent 420179 (1890).
8. A. M. Dollar, H. Herr, Lower extremity exoskeletons and active orthoses: Challenges and state-of-the-art. *IEEE T. Robot.* **24**, 144–158 (2008).
9. S. H. Collins, M. B. Wiggin, G. S. Sawicki, Reducing the energy cost of human walking using an unpowered exoskeleton. *Nature* **522**, 212–215 (2015).
10. W. Hoogkamer, S. Kipp, J. H. Frank, E. M. Farina, G. Luo, R. Kram, A comparison of the energetic cost of running in marathon racing shoes. *Sports Med.* **48**, 1009–1019 (2018).
11. R. Nasiri, A. Ahmadi, M. N. Ahmadabadi, Reducing the energy cost of human running using an unpowered exoskeleton. *IEEE T. Neur. Sys. Reh.* **26**, 2026–2032 (2018).
12. A. M. Grabowski, H. M. Herr, Leg exoskeleton reduces the metabolic cost of human hopping. *J. Appl. Physiol.* **107**, 670–678 (2009).
13. P. G. Weyand, M. W. Bundle, C. P. McGowan, A. Grabowski, M. B. Brown, R. Kram, H. Herr, The fastest runner on artificial legs: Different limbs, similar function? *J. Appl. Physiol.* **107**, 903–911 (2009).
14. P. G. Weyand, D. B. Sternlight, M. J. Bellizzi, S. Wright, Faster top running speeds are achieved with greater ground forces not more rapid leg movements. *J. Appl. Physiol.* **89**, 1991–1999 (2000).

15. P. Holmes, R. J. Full, D. Koditschek, J. Gückenheimer, The dynamics of legged locomotion: Models, analyses, and challenges. *SIAM Rev.* **48**, 207–304 (2006).
16. M. Ilton, M. S. Bhamla, X. Ma, S. M. Cox, L. L. Fitchett, Y. Kim, J.-s. Koh, D. Krishnamurthy, C.-Y. Kuo, F. Z. Temel, A. J. Crosby, M. Prakash, G. P. Sutton, R. J. Wood, E. Azizi, S. Bergbreiter, S. N. Patek, The principles of cascading power limits in small, fast biological and engineered systems. *Science* **360**, eaao1082 (2018).
17. A. V. Hill, The air-resistance to a runner. *Proc. R. Soc. Lond. B* **102**, 380–385 (1928).
18. R. Blickhan, The spring-mass model for running and hopping. *J. Biomech.* **22**, 1217–1227 (1989).
19. T. A. McMahon, G. C. Cheng, The mechanics of running: How does stiffness couple with speed? *J. Biomech.* **23**, 65–78 (1990).
20. A. Arampatzis, G.-P. Brüggemann, V. Metzler, The effect of speed on leg stiffness and joint kinetics in human running. *J. Biomech.* **32**, 1349–1353 (1999).
21. J. Zhang, P. Fiers, K. A. Witte, R. W. Jackson, K. L. Poggensee, C. G. Atkeson, S. H. Collins, Human-in-the-loop optimization of exoskeleton assistance during walking. *Science* **356**, 1280–1284 (2017).
22. A. Sutrisno, D. J. Braun, Enhancing mobility with quasi-passive variable stiffness exoskeletons. *IEEE T. Neur. Sys. Reh.* **27**, 487–496 (2019).
23. W. J. Schwind, D. E. Koditschek, Approximating the stance map of a 2-DOF monoped runner. *J. Nonlinear Sci.* **10**, 533–568 (2000).
24. H. Geyer, A. Seyfarth, R. Blickhan, Compliant leg behavior explains basic dynamic of walking and running. *Proc. R. Soc. B* **273**, 2861–2867 (2006).
25. J.-B. Morin, M. Bourdin, P. Edouard, N. Peyrot, P. Samozino, J.-R. Lacour, Mechanical determinants of 100-m sprint running performance. *Eur. J. Appl. Physiol.* **112**, 3921–3930 (2012).
26. S. Dorel, C. A. Hautier, O. Rambaud, D. Rouffet, E. Van Praagh, J.-R. Lacour, M. Bourdin, Torque and power-velocity relationship in cycling: Relevance to track sprint performance in world-class cyclists. *Int. J. Sports Med.* **26**, 739–746 (2005).
27. M. Garcia, A. Chatterjee, A. Ruina, M. Coleman, The simplest walking model: Stability, complexity, and scaling. *J. Biomech. Eng.* **120**, 281–288 (1998).
28. D. J. Braun, V. Chalvet, T.-H. Chong, S. S. Apte, N. Hogan, Variable stiffness spring actuators for low-energy-cost human augmentation. *IEEE T. Robot.* **35**, 1435–1449 (2019).
29. E. M. Glanzer, P. G. Adamczyk, Design and validation of a semi-active variable stiffness foot prosthesis. *IEEE T. Neur. Reh.* **26**, 2351–2359 (2018).
30. T. Sugar, K. Hollander, Adjustable stiffness Jack-Spring actuator, U.S. Patent 7992849B2 (2011).
31. V. Chalvet, D. J. Braun, Criterion for the design of low-power variable stiffness mechanisms. *IEEE T. Robot.* **33**, 1002–1010 (2017).
32. D. J. Braun, V. Chalvet, A. Dahiya, Positive–negative stiffness actuators. *IEEE T. Robot.* **35**, 162–173 (2019).
33. H. F. Lau, A. Sutrisno, T. H. Chong, D. J. Braun, Stiffness modulator: A novel actuator for human augmentation, in *2018 IEEE International Conference on Robotics and Automation (ICRA)* (IEEE, 2018), pp. 7742–7748.
34. S. Collins, A. Ruina, R. Tedrake, M. Wisse, Efficient bipedal robots based on passive-dynamic walkers. *Science* **307**, 1082–1085 (2005).
35. S.-Y. Fu, B. Lauke, E. Mäder, C.-Y. Yue, X. Hu, Tensile properties of short-glass-fiber- and short-carbon-fiber-reinforced polypropylene composites. *Compos. Part A Appl. Sci. Manuf.* **31**, 1117–1125 (2000).
36. G.-P. Brüggemann, A. Arampatzis, F. Emrich, W. Potthast, Biomechanics of double transtibial amputee sprinting using dedicated sprinting prosthesis. *Sports Technol.* **1**, 220–227 (2008).
37. G. Elliot, G. S. Sawicki, A. Marecki, H. Herr, The biomechanics and energetics of human running using an elastic knee exoskeleton, in *2013 IEEE 13th International Conference on Rehabilitation Robotics* (ICORR) (IEEE,, 2013), pp. 1–6.
38. M. S. Cherry, S. Kota, D. P. Ferris, Running with an elastic lower limb exoskeleton. *J. Appl. Biomech.* **32**, 269–277 (2016).
39. J. L. Pons, *Wearable Robots: Biomechatronic Exoskeletons* (John Wiley & Sons, 2008).
40. L. Li, How can sport biomechanics contribute to the advance of world record and best athletic performance. *Meas. Phys. Ed. Exerc. Sci.* **16**, 194–202 (2012).
41. A. Seyfarth, H. Geyer, M. Günther, R. Blickhan, A movement criterion for running. *J. Biomech.* **35**, 649–655 (2002).
42. H. Geyer, A. Seyfarth, R. Blickhan, Spring-mass running: Simple approximate solution and application to gait stability. *J. Theor. Biol.* **232**, 315–328 (2005).
43. M. Srinivasan, A. Ruina, Computer optimization of a minimal biped model discovers walking and running. *Nature* **439**, 72–75 (2006).
44. P. E. di Prampero, S. Fusi, L. Sepulcri, J. B. Morin, A. Belli, G. Antonutto, Sprint running: A new energetic approach. *J. Exp. Biol.* **208**, 2809–2816 (2005).
45. K. P. Clark, P. G. Weyand, Are running speeds maximized with simple-spring stance mechanics? *J. Appl. Physiol.* **117**, 604–615 (2014).
46. S. H. Patterson, Bicycle gear shifting method and apparatus, U.S. Patent 4900291 (1990).
47. J. Gückenheimer, P. Holmes, *Nonlinear Oscillations, Dynamical Systems and Bifurcation of Vector Fields* (Springer-Verlag, 1983).
48. C. Capelli, F. Schena, P. Zamparo, A. D. Monte, M. Faina, P. E. di Prampero, Energetics of best performances in track cycling. *Med. Sci. Sports Exerc.* **30**, 614–624 (1998).
49. R. P. Patterson, M. I. Moreno, Bicycle pedalling forces as a function of pedalling rate and power output. *Med. Sci. Sports. Exerc.* **22**, 512–516 (1990).
50. C. E. Clauser, J. T. McConville, J. W. Young, Weight, volume, and center of mass of segments of the human body (Report AD-170 622, Wright-Patterson Air Force Base, 1969).
51. R. V. Brulee, *Engineering the Space Age: A Rocket Scientist Remembers* (Air Univ. Press, 2008).
52. Speed-skating world records, Men's 500 m (2015). Accessed on 23 August 2019; http://www.speedskatingstats.com/index.php?file=records&g=m&event=500.
53. R. Hymans, I. Matrahazi, Progression of IAAF world records (2015). Accessed on 23 August 2019; http://iaaf-ebooks.s3.amazonaws.com/2015/Progression-of-IAAF-World-Records-2015/projet/IAAF-WRPB-2015.pdf.

Acknowledgments

Funding: The authors received institutional support from Vanderbilt University in support of this research. **Author contributions:** D.J.B. and A.S. conceived the method, developed the theory, derived the supporting equations, and wrote the manuscript. A.S. performed the numerical simulations. D.J.B. reviewed the manuscript. Both authors approved the final manuscript. **Competing interests:** D.J.B. and A.S. are inventors on a pending patent related to this work filed by Vanderbilt University (no. 62/950,641, filed on 19 December 2019). The authors declare no other competing interests. **Data and materials availability:** All data needed to evaluate the conclusions in the paper are present in the paper and/or the Supplementary Materials.

Submitted 28 May 2019
Accepted 3 January 2020
Published 25 March 2020
10.1126/sciadv.aay1950

Citation: A. Sutrisno, D. J. Braun, How to run 50% faster without external energy. *Sci. Adv.* **6**, eaay1950 (2020).

Science Advances

How to run 50% faster without external energy

Amanda Sutrisno and David J. Braun

Sci Adv **6** (13), eaay1950.
DOI: 10.1126/sciadv.aay1950